Testing the ability of 2-dimensional vortex methods to reproduce simulations of nearly inviscid vortex dynamics

Kieran Bhatia
Rosenstiel School of Marine and Atmospheric Science
University of Miami, Miami, Florida, US

1) Introduction

In two dimensions, vorticity is materially conserved in an invisicid environment. Additionally, if the fluid is non-divergent, the velocity field can be determined from a solution to the Poisson equation relating velocity and vorticity. Vortex methods translate these well-known facts as well as the ability to capture the time evolution of Lagrangian particles into a method of representing the flow evolutions of initially defined vorticity fields (Leonard 1980). Although vortex methods are now also used to model the development of three-dimensional flows with or without viscosity, they evolved from the adherence to two fundamental equations.

$$\frac{\mathrm{d}\omega}{\mathrm{d}t} = \frac{\partial\omega}{\partial t} + \mathbf{u}\cdot\nabla\omega = 0 \quad (1)$$

$$\nabla^2\psi = -\omega \quad (2)$$

In 1931, vortex methods were utilized for the first time by Rosenhead, who reproduced the motion of a two-dimensional vortex sheet by calculating the induced movement from a collection of point vortices (Leonard 1980). Almost forty years later, Dushane (1973) and Chorin (1973) published influential results which proved that “blobs” or patches of vorticity more accurately represented vorticity fields than points. Dushane and Chorin showed that unlike point vortices which approximate vorticity with delta functions, the cutoff function representing the vorticity and velocity distribution within blobs does not contain a singularity in the vicinity of the blob center. At the same time, these cutoff functions display the behavior of a point vortex away from the center. Since then, countless studies have simulated two-dimensional flows by discretizing areas of vorticity with blobs and monitoring the time evolution of the location of the blobs to reproduce real-world processes. However, vortex methods have received little attention in two-dimensional simulations of the evolution of hurricane-like vortices. The lack of discussion of vortex methods in this context is particularly surprising when considering the amount of studies employing 2D finite difference and spectral models to conduct numerical simulations of barotropic vortices. Two such simulations were carried out by Schubert et al. (1999, hereafter SM99) and Hendricks et al. (2009, hereafter HS09).

SM99 conducted numerical experiments involving an initial vorticity distribution which consisted of an annulus of high vorticity surrounding a region of lower vorticity. This configuration aimed to represent the vorticity structure associated with hurricane-like vortices. SM99 ran their experiments with an unforced pseudospectral barotropic nondivergent model with constant viscosity. They acknowledged their results cannot capture the true dynamics of hurricanes because of the omission of moist physical processes and the lack of a vertical structure in their model. Yet, SM99 highlights the realistic nature of their model’s simulation of certain tropical cyclone dynamics, such as barotropic instabilities. Throughout their study, SM99 investigate how two particular parameters: gamma (ratio of inner region vorticity to average vorticity) and delta (annulus ring thickness) affect the stability of the initial vortex and the end state. A particular gamma-delta combination is shown in their “representative numerical

experiment" for which they list the initial condition parameters as well as the vorticity contour plots up to 48 hours. An equivalent vortex methods simulation is performed by applying these initial parameters and compared to the SM99 vorticity contour plots.

The other numerical simulation reproduced here with vortex methods was conducted by HS09. HS09 summarized the results from 170 numerical simulations produced by a similar model to SM99, and the end states (at 48 hours) were explained based on the same parameters gamma and delta from SM99. A unique set of simulations run by HS09 involve hollow vortices with thin rings (large delta, small gamma), where the end state contains mesovortices which in some cases, persist indefinitely. HS09 includes images at 0, 1, and 48 hours for different cases of high vorticity annuli evolving into mesovortices. The delta and gamma from a particular simulation are used as initial conditions for vortex blob methods, and the results are compared to the images produced by the pseudosprectral model in HS09. It is hypothesized that two-dimensional vortex methods can reproduce similar 2D phenomena that are resolved with the simple model used in SM99 and HS09.

2) Methodology

The numerical model used to reproduce the results from HS09 and SM99 is a two-dimensional incompressible flow model which relies on two-dimensional vortex methods. A major difference between vortex methods and the pseudosprectral model in HS09 and SM99 comes from the treatment of the vorticity transport equation (eqn. 1). Unlike spectral methods, the transport equation is dealt with exactly in vortex methods, and the only shortcoming comes from the slight imprecision of replacing the initial vorticity by the correct distribution of blobs and representing the radial profile of the velocity and vorticity of the blob (cutoff function) (Cottet 2000). Both HS09 and SM99 explicitly detail the initial vorticity distribution which prescribes blob strength and location. However, the blob cutoff function for the vorticity and associated velocity kernel, blob width, and amount of blobs are adjustable.

The chosen order (n) of the cutoff function describing the blob vorticity and velocity profile determines how well (up to order n-1) the blobs represent point vortices (Cottet 2000). As a result, cutoff functions of the second, fourth, and sixth order (Fig. 1) were tested to monitor how their order affected results (Hald 1991). Additionally, varying blob amounts with the corresponding blob widths were also tested with the intention of gaining more accurate results. Once the initial conditions are set, the velocity field induced by all vortex blobs on all other blobs is determined and as time moves on, blob position is updated by integrating the equation for blob motion using a Runge-Kutta 4 integrator (Leonard 1980).

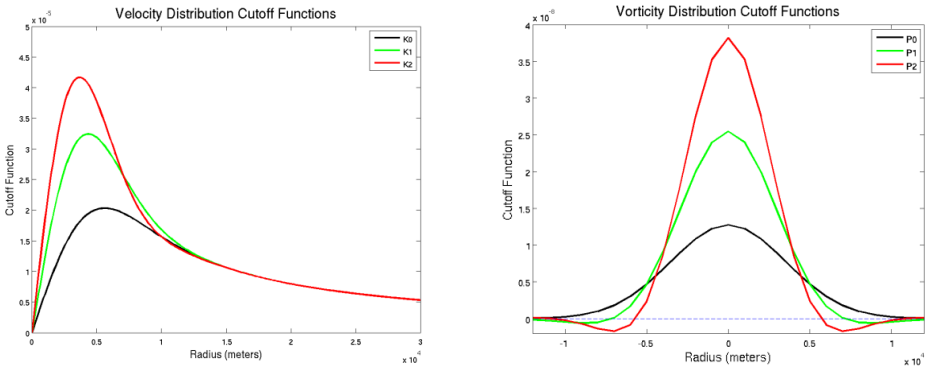

Fig. 1. Velocity and Vorticity cutoff functions where K0, P0= 2nd order; K1, P1=4th order; and K2, P2=6th order

3) Tests and Results

a. Schubert Et Al. Representative Vortex

The particular case in SM99 analyzed using 2D vortex methods was the representative numerical experiment with the following initial conditions: γ =0.2, r_1=37.5 kilometers, r_2=57.5 kilometers (corresponds to a δ=0.652), ζ_1 =3.576 *10^{-4} s^{-1}, ζ_2= 3.285*10^{-3} s^{-1}, and a maximum tangential wind of 54 m/s near the outer ring radius. SM99 mentions that the wavenumber 4 is the most unstable with an e-folding time of 57.5 minutes. All of these parameters were inputted into the initial state for the vortex methods simulation and the initial high vorticity ring was accurately duplicated. Thirty-two different vortex methods simulations utilizing different combinations of blob size, blob width, and blob cutoff functions were attempted to best reproduce the SM99 vortex. Blob amounts ranging from 4,000 to 15,000 were used with blob widths ranging from 1 to 7 kilometers. Additionally, all three cutoff functions (P0 to P2 and K0 to K2 or 2nd to 6th order) were used. From in-depth qualitative analysis, the best vortex methods simulation incorporated 12,000 blobs, with 2 kilometer wide blobs, and blob velocity and vorticity distributions described by a fourth order cutoff function. Even though the flow field generally appears consistent for a wide range of blob values, the larger blob amounts better resolve the small-scale motions that are visible in the SM99 images. Therefore, the 12,000 blobs with 2 kilometer width scenario produced a good compromise between computer speed and accuracy; still, the further accuracy of more blobs warrants increasing the quantity of blobs in future work to see how results are altered.

The results of the vortex methods experiments are displayed in the form of vorticity plots for a 24 hour period with 2 hour increments (Fig. 2) (see Fig.3. in SM99 for comparison). Initially, both the SM99 and vortex methods vorticity distributions contain a low vorticity inner region with a high vorticity ring. By hour 2, the vortex methods plot portrays localized areas of high vorticity forming near the boundary between the annulus and center. The vorticity values of these maxima are larger than the original maximum vorticity because the overlap of many blobs causes unphysical vorticity values. As barotropic instabilities develop, the low vorticity center mixes with the high vorticity ring. At four hours, the vortex methods simulation produces a clear wavenumber 4 pattern in the eyewall which is almost identical to the SM99 vorticity distribution. By comparing the hour four plots, it is clear the most unstable mode growth is larger for the vortex methods case. This observation of a discrepancy in growth rate becomes more apparent in the hour 6 plots where the spiral bands are starting to form for the vortex methods simulation but the SM99 vortex shows little deformation in the annulus. The low vorticity center reduces in size similarly for both simulations up until 12 hours where the two simulations begin to differ more noticeably from each other. By 14 hours in Fig. 2. , the remaining low vorticity patch has moved to the outside and is significantly smaller while the SM99 hour 14 vorticity distribution shows a low vorticity region that is closer to the center and larger. The discrepancy between the two simulations is also visible in the vortex methods vorticity profile which is clearly monotonic at 24 hours while the SM99 vorticity profile has not reached a monopolar configuration (Fig. 3). Although the vortex methods model is depicting an instability that is growing faster than the SM99 case, there is evidence from Kossin and Eastin's (2001) results that a shorter time period to reach a monotonic vorticity profile is observed for actual storms. A simple growth rate calculation should demonstrate that the qualitative analysis demonstrating differing growth rates is well-grounded.

In SM99, the authors derive a dimensionless growth rate (SM99 eqn. 2.11) that depends on gamma, delta, and m (the

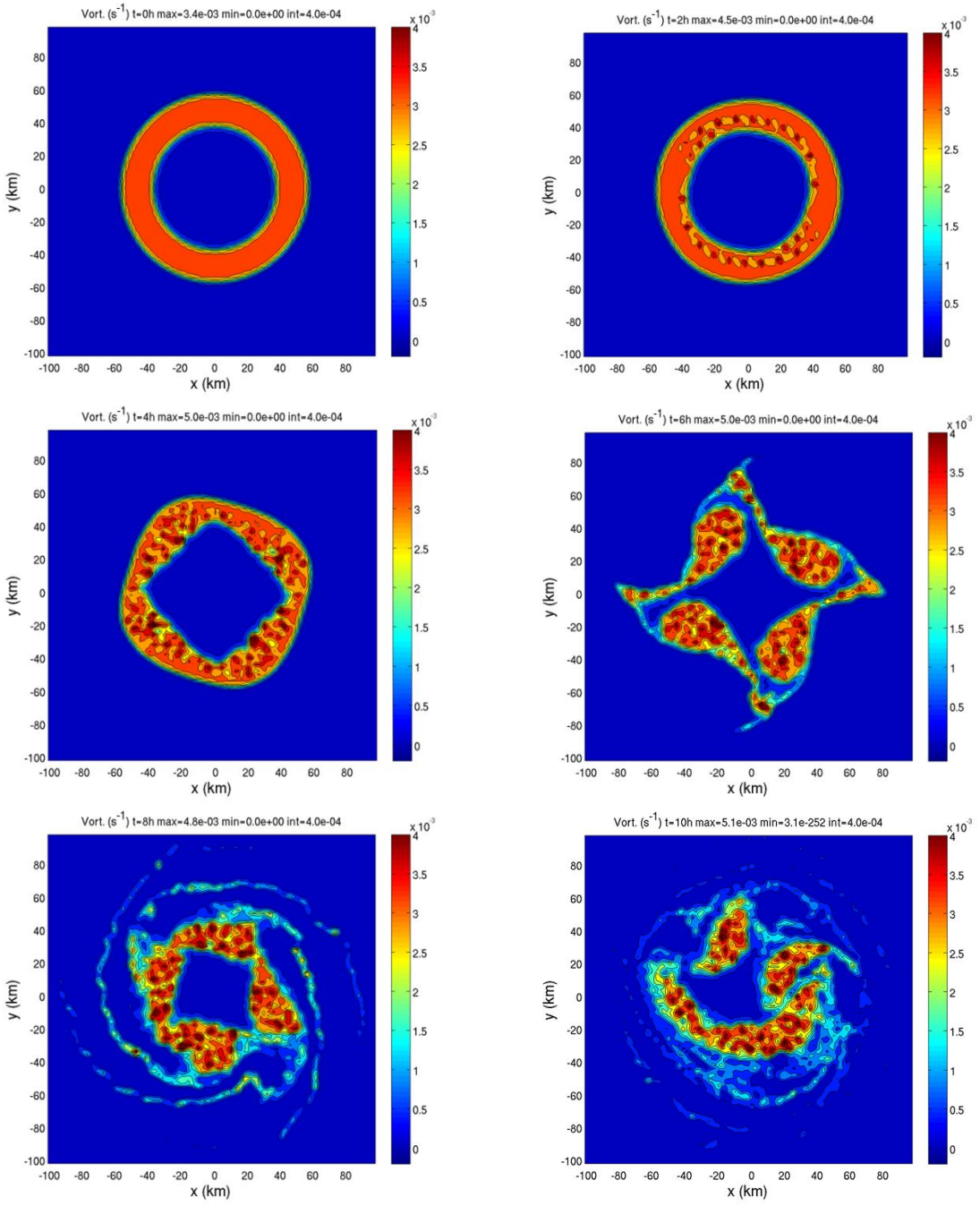

Fig. 2. Vorticity contour plots for the 2D vortex methods representation of the representative numerical experiment from SM 99. Low vorticity values are shaded blue and high vorticity values are shaded red. (a) Vorticity from t=0 hours to 10 hours (every 2 hours).

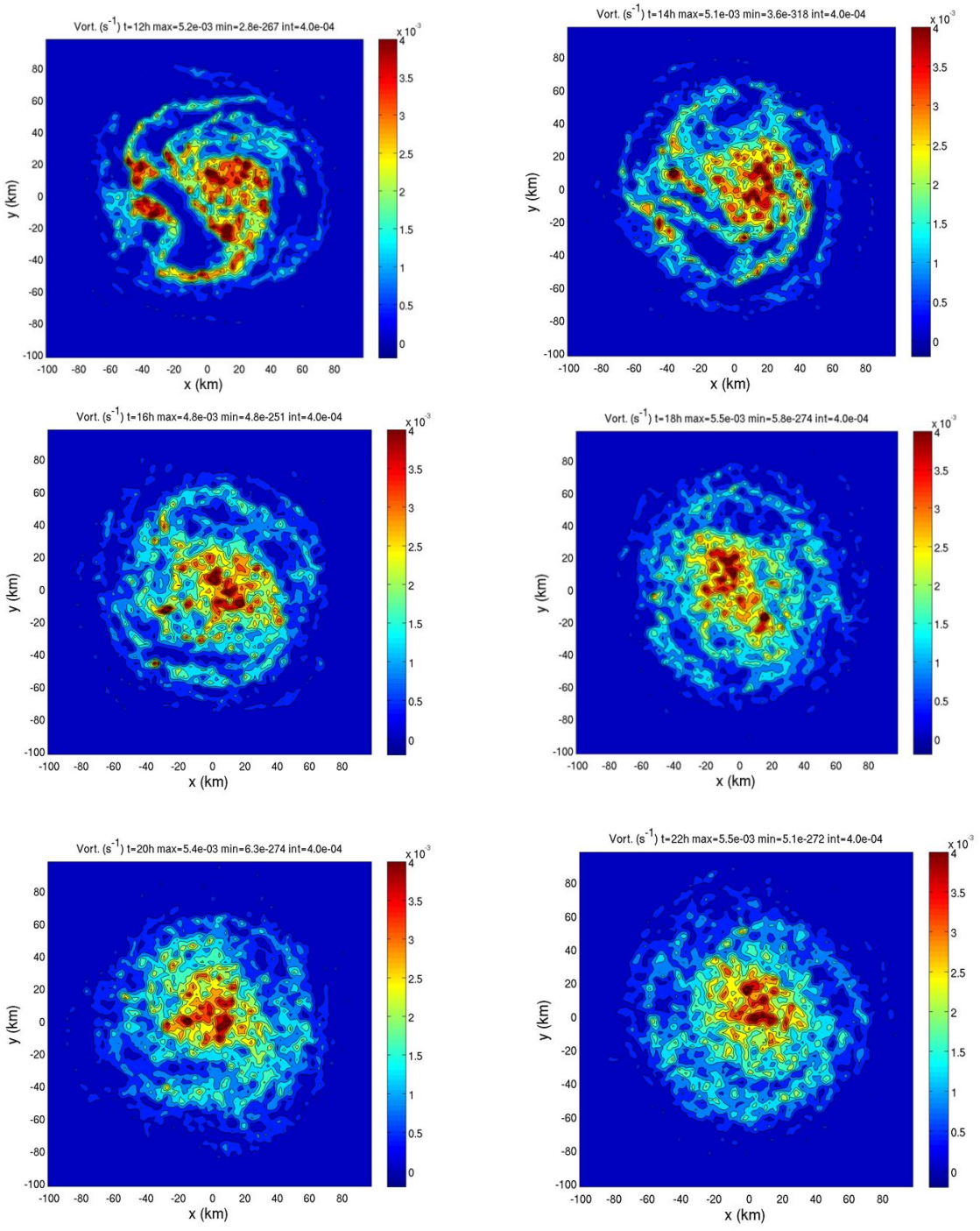

Fig. 2. (Continued) (b) Vorticity from t =12 to 22 hours. 24 hour output not shown because it appears almost identical to 22 hours.

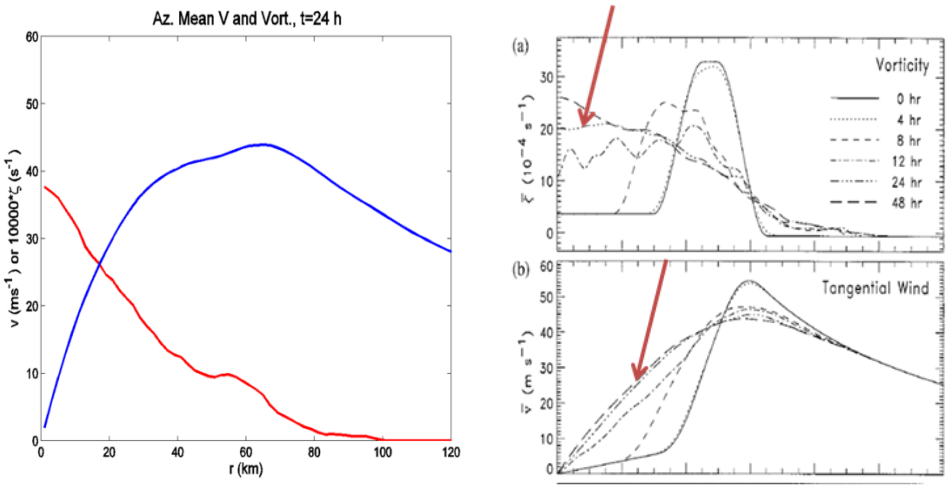

Fig. 3. (Left) Profile of vorticity (red) and tangential wind (blue) as a function of radius at 24 hours for the vortex methods case. (Right) Vorticity and tangential wind for the SM99 case. The red arrow indicates the hour 24 data.

disturbance tangential wavenumber). The vortex methods analysis is not governed by the same equation because it does not contain the same discontinuous piecewise vorticity profile, excludes viscosity, and contains smooth transitions between the different vorticity regimes (annulus, center, and exterior).

Therefore, other properties of the flow need to be used to come up with a growth rate. The fact that there is no radial component of the initial velocity profile conveys that any radial component of velocity as time progresses is a result of a perturbation. The fastest growing perturbation represents the most unstable mode which dominates during the growth of the instability. Therefore, the steepest slope of the log(radial velocity) versus time plot will yield the dimensional growth rate. Though, the value obtained for the largest rise in radial velocity versus time depends on the length of the time interval chosen. By analyzing several plots of log(radial velocity) as a function of time, the logarithmic growth period of the instability occurs during the first three hours. Further investigation demonstrates all vortex methods simulations obtain an even faster sustained growth period during a time range between 90 minutes and 120 minutes. In figure 4, growth rates are listed for the 6000 blob case for all three cutoff functions by calculating the one hour and 10 minute maximum slopes. These growth rates are translated into e-folding times and compared to the SM99 listed growth rate. It is clear that defining the correct time period to calculate the growth rate is important to the results but choosing that time range is, to a degree, subjective. However, from qualitative analysis of Fig. 2, the shorter e-folding times seem more reasonable. Possible explanations for the faster growth rate in the vortex methods simulations are the lack of a diffusion term which is present in the SM99 equations. Kossin and Schubert (2001) worked with similar high vorticity annulus distributions and observed an increase in viscosity typically lengthened e-folding times substantially.

Cutoff Function	Dimensional Growth Rate from 10 minute slopes (1/hr)	E-folding time (Minutes)	Dimensional Growth Rate from hour slope	E-folding time (minutes)	SM99 e-folding time (minutes)
P0 (2nd order)	1.65	36.46	0.800	75.0	57.5
P1 (4th order)	2.11	28.39	1.089	55.1	
P2 (6th order)	2.14	28.07	1.142	52.5	

Table 1. Dimensional growth rates and e-folding times computed from the maximum slope of a log(radial velocity) vs. time plot during the logarithmic growth period for 10 minute and hour time steps.

b. Hendricks Et Al. (δ, γ) = (0.85, 0.10) Vortex

The particular numerical simulation from HS09 analyzed with 2D vortex methods was the (δ, γ) = (0.85, 0.10) vortex with the following initial conditions: r_1=34 kilometers, r_2=40 kilometers, ζ_1=2.000 *10^{-4} s^{-1}, ζ_2= 6.686*10^{-3} s^{-1}, and a maximum tangential wind of 40 m/s near the outer ring radius. These parameters defined the 0 hour vortex that was modeled with 2D vortex methods. Additionally, a broadbanded perturbation (obtained from HS09) was applied to the annulus to mimic the naturally occurring random noise that creates instability in real hurricanes. Sixteen different vortex methods simulations utilizing different combinations of blob size, blob width, and blob cutoff functions were run with the intention of replicating the evolution of the particular HS09 vortex. Blob amounts ranging from 6,000 to 12,000 were tested with blob widths ranging from 2 to 6 kilometers. Again, experiments considered three cutoff functions (P0 to P2 and K0 to K2 or 2nd to 6th order). Qualitatively, the best vortex methods simulation included 12,000 blobs with a blob width of 3 kilometers and blob velocity and vorticity distributions described by a sixth order cutoff function. Unlike the SM99 simulations, the HS09 vortex development was very sensitive to changes in blob width, amount, and cutoff function. In general, larger amounts of blobs and higher order cutoff function led to less mesovortices in the end state.

HS09 notes that the most unstable wavenumber for the (δ, γ)=(0.85, 0.10) vortex is 6 and the final state (at 48 hours) of the vorticity distribution contains four mesovortices. The 2D vortex methods experiments never yielded an end state of 4 mesovortices or the most unstable wavenumber of 6. For the most representative vortex methods simulation, 5 mesovortices were observed at 48 hours with a most unstable wavenumber of 7 (Fig. 4.). However, in general, the vortex methods simulations display many of the same properties as the pseudospectral model results from HS09. Both HS09 and vortex methods demonstrate certain thin annuli quickly “roll up” into mesovortices, experience merger events, and do not consolidate into monopoles. The vortex methods and HS09 experiments produce mesovortices that form a rigid configuration that rotates as a solid body. Similar asymmetric steady solutions are observed in laboratory experiments using electron plasmas, and have been named “vortex crystals” (Kossin and Schubert 2001).

Still, it is important to discuss the potential reasons for the differing final states

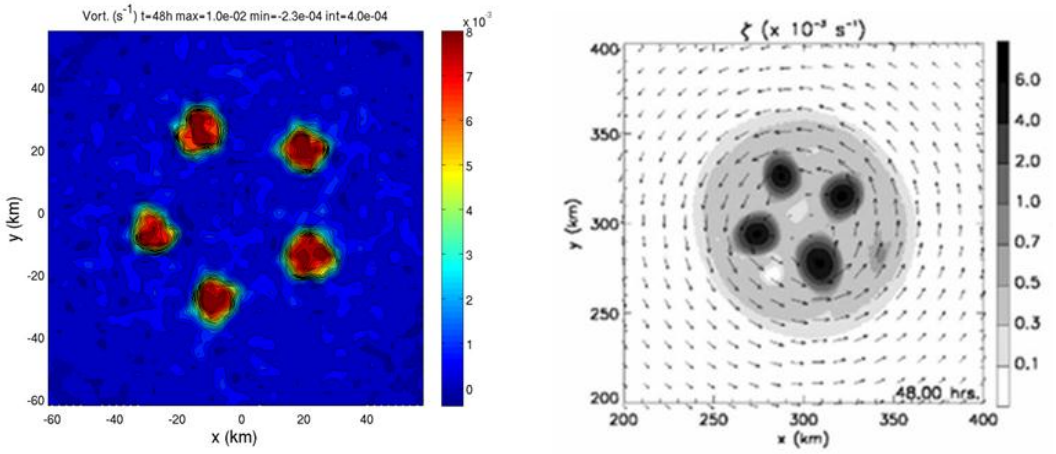

Fig. 4. End states (48 hours) for the 2D vortex methods simulation (left) and HS09 simulation (right)

of the HS09 and vortex methods simulation. Schecter et al. (1999) studied the evolution of high vorticity annuli similar to the (δ, γ) =(0.85, 0.10) HS09 case by comparing experiments on magnetized electron columns with vortex methods simulations. His results indicated that viscosity in the Navier–Stokes equations weakens mesovortices and moderates the vorticity distribution. In fact, high levels of viscosity can expand mesovortices fast enough to encourage multiple mergers before they have time to settle into vortex crystal geometry (Schecter et al. 1999). Additionally, simulations with smaller and more blobs are necessary to further improve the accuracy of the 2D vortex methods.

4. Discussions and Conclusions

This study used 2D inviscid vortex methods to represent the development of two vorticity distributions characterized by an annulus of higher vorticity surrounding a region of lower vorticity. The two reference experiments were obtained from the representative numerical experiment from SM99 and the (δ, γ) =(0.85, 0.10) vortex from HS09. The 2D vortex simulations experiments and reference experiments yield qualitatively similar results. The vortex methods model reproduced many of the same 2D phenomena observed in the SM99 and HS09 simulations. In the SM99 best vortex methods simulation, the dominant mode-4 disturbance is apparent at early times, and the interactions between the low vorticity core and high vorticity ring are reminiscent of the SM99 plots. Yet, a more detailed assessment indicates a significant growth rate discrepancy between the two models (Table 1). Fig. 3 suggests the vortex method simulation reaches a monotonic vorticity profile well before the SM99 experiment. The exact difference between the growth rates is unclear due to the mentioned (section 3a.) subjective nature of the calculation of the values in table 1. Nevertheless, the discrepancy in the results can be attributable to the SM99 model including a constant viscosity while the vortex methods do not.

Also, the lack of viscosity appears to affect the results of the 2D vortex methods simulation of the HS09 vortex. At 48 hours, the HS09 model produces four mesovortices while the vortex methods model contains five. Additionally, the most unstable mode does not agree for the two simulations. Work by Schecter et al. (1999) suggests including viscosity could significantly alter the vortex methods end state. The simplest way to incorporate viscosity into the 2D vortex methods models is to add a slight random walk to each blob during the simulation. Once this is accomplished, the effect of a basic viscosity on the vortex methods model will be present, hopefully producing an end state

similar to HS09. There are a number of other potential explanations for the inconsistency between the HS09 and vortex method results. One possible solution involves increasing the number of blobs and decreasing the blob width to increase the "resolution" of the vortex methods.

By comparing the 2D vortex methods simulations to the SM99 and HS09 studies, 2D vortex methods appear to accurately capture the general features of the flow evolution of hurricane-like vortices. The 2D vortex methods satisfy the inviscid equations of motion exactly so they are a useful tool for capturing barotropic processes that are common in hurricanes. With the mentioned updates to the 2D vortex methods model, it is hypothesized that the HS09 and SM99 case studies would be better replicated by the vortex methods.

5. References

Beale, J.T., and A.J. Majda (1985). High order accurate vortex methods with explicit velocity kernels. *J. Comput. Phys*., **58**, p. 188

Cottet G.-H. and P. Koumoutsakos, Vortex Methods: Theory and Practice (Cambridge Univ. Press, Cambridge, UK, 1999).

Chorin, A. J., Numerical study of slightly viscous flows, *J. Fluid Mech.*, **57** (1973), 785-796.

Dushane, T. E. Convergence of a vortex method for solving Eider's equation, *Math. Comp*., **27** (1973), 719.

Hald, Ole. Vortex methods and vortex motion (A91-30351 11-34). Philadelphia, PA, *Society for Industrial and Applied Mathematics*, 1991, p. 33-58.

Hendricks, E. A., Schubert, W. H., Taft, R. K., Wang, H., & Kossin, J. P. (2009). Life Cycles of Hurricane-Like Vorticity Rings. *J. Atmos. Sci.*, **66**(3), 705-72.

Kossin, J., and W. H. Schubert, 2001: Mesovortices, polygonal flow patterns, and rapid pressure falls in hurricane-like vortices. *J. Atmos. Sci*., **58**, 2196–2209.

Kossin, J. P., and M. D. Eastin, 2001: Two distinct regimes in the kinematic and thermodynamic structure of the hurricane eye and eyewall. *J. Atmos. Sci*., **58**, 1079-1090.

Leonard, A. (1980) Vortex Methods for Flow Simulations. *J. Comput. Phys.,* **37,** 289-335.

Schecter, D. A., D. H. E. Dubin, K. S. Fine, and C. F. Driscoll, 1999: Vortex crystals from 2D flow: Experiment and simulation. *Phys. Fluids*, **11**, 905–914.

Schubert, W. H., and Montgomery, M. T. (1999). Polygonal Eyewalls, Asymmetric Eye Contraction, and Potential Vorticity Mixing in Hurricanes. *J. Atmos. Sci*., **56**(9), 1197.